Title

Delivery of siRNA via cationic Sterosomes to enhance osteogenic differentiation of mesenchymal stem cells

Authors

Cui, Zhong-Kai

Fan, Jiabing

Kim, Soyon

et al.

Publication Date

2015-11-01

DOI

10.1016/j.jconrel.2015.08.031

Peer reviewed

HHS Public Access

Author manuscript

J Control Release. Author manuscript; available in PMC 2016 November 10.

Published in final edited form as:

J Control Release. 2015 November 10; 217: 42–52. doi:10.1016/j.jconrel.2015.08.031.

Delivery of siRNA via cationic Sterosomes to enhance osteogenic differentiation of mesenchymal stem cells

Zhong-Kai Cui[1], **Jiabing Fan**[1], **Soyon Kim**[2], **Olga Bezouglaia**[3], **Armita Fartash**[3], **Benjamin M. Wu**[1,2], **Tara Aghaloo**[3], and **Min Lee**[1,2,*]

[1]Division of Advanced Prosthodontics, University of California Los Angeles, 10833 Le Conte Avenue, Los Angeles, CA 90095

[2]Department of Bioengineering, University of California Los Angeles, 420 Westwood Plaza, Los Angeles, CA 90095

[3]Division of Diagnostic and Surgical Sciences, University of California Los Angeles, 10833 Le Conte Avenue, Los Angeles, CA 90095

Abstract

Noggin is a specific antagonist of bone morphogenetic proteins (BMPs) that can prevent the interaction of BMPs with their receptors. RNA interfering molecules have been used to downregulate noggin expression and thereby stimulate BMP signaling and osteogenesis. Cationic liposomes are considered one of the most efficient non-viral systems for gene delivery. In the past decade, non-phospholipid liposomes (Sterosomes) formulated with single-chain amphiphiles and high content of sterols have been developed. In particular, Sterosomes composed of stearylamine (SA) and cholesterol (Chol) display distinct properties compared with traditional phospholipid liposomes, including increased positive surface charges and enhanced particle stability. Herein, we report SA/Chol Sterosome and small interfering RNA (siRNA) complexes that significantly enhanced cellular uptake and gene knockdown efficiencies in adipose derived mesenchymal stem cells with minimal cytotoxicity compared with commercially available lipofectamine 2000. Furthermore, we confirmed osteogenic efficacy of these Sterosomes loaded with noggin siRNA in *in vitro* two- and three-dimensional settings as well as in a mouse calvarial defect model. The delivery of siRNA via novel SA/Chol Sterosomes presents a powerful method for efficient gene knockdown. These distinct nanoparticles may present a promising alternative approach for gene delivery.

Graphical Abstract

*Corresponding author. Tel: +1 310 825 6674, Fax: +1 310 825 6345, leemin@ucla.edu.

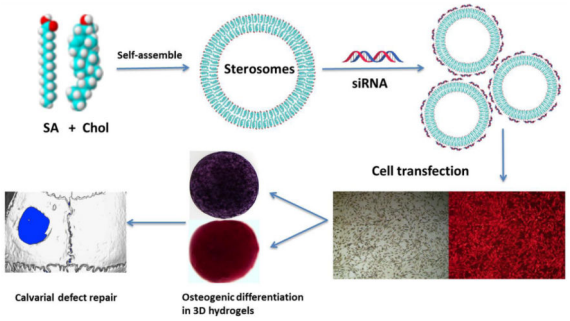

Keywords

Stearylamine; Cholesterol; Sterosomes; siRNA; Mesenchymal stem cells; Osteogenic differentiation

1. Introduction

Gene-based therapies have been extensively investigated to treat diseases by delivering nucleic acids into cells to induce or silence specific gene expression [1-3]. Since the discovery of the RNA interference (RNAi) in 1998 [4], it has been widely used for treating genetic diseases and cancers[5-7] or tissue engineering applications by a delicate control of gene expression and directing stem cell differentiation [8, 9]. In particular with respect to bone tissue engineering, small interfering RNA (siRNA) molecules have been used to downregulate expression of noggin, a specific antagonist of bone morphogenetic proteins (BMPs) that can prevent the interaction of BMPs with their receptors, to enhance osteogenesis *in vitro* as well as bone formation *in vivo* [10-12]. Our previous studies showed that knockdown of noggin expression enhanced both osteogenic differentiation of adipose derived mesenchymal stem cells (ASCs) *in vitro* [13] and bone formation in a mandibular defect model [14]. However, many physiological barriers exist in the delivery of siRNA to the cytoplasm of targeted cells due to their large size, anionic nature and stability. Although viral vectors have advanced in the field of gene delivery, their potential use in clinics are limited due to some disadvantages [15-17]. Lentiviral and adenoviral vectors can cause immune responses [18] and infect non-targeted cells [19], and are relatively difficult to be produced from wild-type virus [20]. Although retroviral viral vectors are relatively low immunogenic, they transduce only replicating cells and there is a high risk of insertional mutagenesis [21]. To overcome these barriers, various delivery systems have been developed for efficient delivery of siRNA using non-viral mediated vehicles [22-25]. Among non-viral delivery systems [8, 16, 24], lipid-based nanoparticles have great potential because of their biocompatibility and low toxicity [26].

Liposomal nanotechnology has significantly evolved and now, liposomes have been applied in many fields including pharmaceutics [27], cosmetics [28], food [29], and textile [30] industries. Liposomes are essentially used as nanocontainers for protecting, transporting and targeting solutes. Cationic liposomes display distinct advantages for some applications related to vectorization and delivery. For instance in gene therapy, cationic liposomes are

reported to interact and complex with DNA, RNA or oligonucleotides, markedly prevent nuclease degradation, facilitate the intracellular uptake and further endosomal escape of oligonucleotide and result in a better intracellular distribution [31-33]. Cationic liposomes are the most common lipid-based nanocarrier used for siRNA delivery.

Recently, it has been reviewed that cholesterol and other sterols can induce the formation of fluid lamellar phases when mixed with single-chain amphiphiles. Even though these single-chain amphiphiles or sterols do not form fluid lamellar phases once hydrated individually, their mixtures lead to stable liquid-ordered bilayers, and the resulting liposomes were named Sterosomes because of the high sterol content [34]. Stearylamine (SA) and cholesterol (Chol) at equimolar ratio form stable large unilamellar vesicles (LUVs) with high positive charge and very limited permeability [35]. Compared to commercially available cationic liposomes such as lipofectamine 2000, we expect that the SA/Chol LUVs could be a better candidate for gene delivery due to their higher positive surface charge and significantly increased particle stability, leading to superior gene knockdown efficiency [35, 36]. In addition, cholesterol was found to have effects on osteoblastic differentiation in mouse mesenchymal stem cells [37].

In this work, we demonstrated the ability of the novel Sterosomes formulated with a single-chain amphiphile SA and high content of Chol to deliver noggin siRNA to enhance osteogenic differentiation of ASCs. First, we evaluated the cytotoxicity of SA/Chol vesicles, characterized their stability under various conditions (e.g. temperature, pH, organic solvent) and determined their complexation efficiency with siRNA. Next, we assessed the cellular uptake efficiency as well as knockdown efficiency of the target gene. We further investigated the ability of SA/Chol Sterosomes loaded with noggin-targeting siRNA to induce osteogenic differentiation of ASCs in two-dimensional (2D) monolayer cell culture as well as in three-dimensional (3D) setting using hydrogels in vitro. Finally, the *in vivo* osteogenic ability of noggin siRNA-loaded Sterosomes was evaluated in a mouse calvarial defect model. This present work demonstrated an alternative method of downregulating gene expression via the designed stable liposomal system for efficient siRNA therapy.

2. Materials and methods

2.1 Materials

Stearylamine (99%), cholesterol (>99%), tris(hydroxymethyl)-aminomethane (TRIS) (99%), NaCl (>99%), Nitro Blue Tetrazolium (NBT), 5-Brom-4-chlor-3-indoxylphosphate (BCIP), Alizarin Red S, L-ascorbic acid, p-nitrophenol phosphate, β-glycerophosphate, dexamethasone, methanol (spectrograde) and benzene (high purity), ethylenediaminetetraacetic acid (EDTA) were purchased from Sigma-Aldrich (St. Louis, MO). Lipofectamine® 2000, Trizol, and cDNA transcription kit, Low Glucose Dulbecco's Modified Eagle's Medium (DMEM), Penicillin/Streptomycin (100 U/ml) (P/S) were obtained from Life Technologies (Grand Island, NY). Fetal Bovine Serum (FBS) was supplied by Mediatech Inc. (Manassas, VA). Noggin and control siRNA were ordered from Santa Cruz Biotechnology (Santa Cruz, CA). RNeasy Mini kit was purchased from Qiagen (Valencia, CA). C57/BL mice and nude mice were supplied from Charles River

Laboratories (Wilmington, MA). All solvents and products were used without further purification.

2.2 Sterosomes preparation

Mixtures of stearylamine and cholesterol were prepared by dissolving weighed amounts of the solid chemicals in a mixture of benzene/methanol 90/10 (v/v). The solutions were then frozen in liquid nitrogen and lyophilized for at least 16 h to allow complete sublimation of the organic solvent.[35] The freeze-dried lipid mixtures were hydrated with a TRIS buffer (TRIS 50 mM, NaCl 140 mM) at pH 7.4. In order to ensure a good hydration of the samples, the suspensions were subjected to five temperature cycles from liquid nitrogen temperature to ~70 °C, and were vortexed between successive cycles. LUVs were prepared by sonication (20 s on and 5 s off, amplitude 20%) for 20 min. The hydrodynamic diameters and the zeta potential of resulting LUVs were measured at 25 °C, using a Malvern Zetasizer.

2.3 siRNA complexation efficiency

Lipoplexes of siRNA and Lipofectamine 2000 were prepared following the protocol provided by the manufacturer. Briefly, mix lipofectamine 2000 with Opti-MEM (Invitrogen) and mix siRNA with Opti-MEM in Eppendorf tubes, respectively, and stand at room temperature for 5 min. Combine the contents of two tubes and incubate at room temperature for 20 min. The final volume is 1 mL with 5 μg/mL lipofectamine 2000 and 100 nM siRNA. The same simple mixing preparation method was used for our Sterosome SA/Chol and siRNA complexes but in a TRIS buffer. Each sample solution was used immediately after preparation. The complexation efficiency of siRNA with the particles was determined using fluorescently labeled siRNA (Cy3-siRNA, Ambion Inc., Austin, TX). After Cy3-siRNA was complexed with the particles as stated above, suspensions were centrifuged at 15 000 rpm for 40 min at 4 °C, and then the amount of residual Cy3-siRNA in the supernatant was measured using fluorescent microplate reader (n = 3). The complexation efficiency (%) was calculated using the following equation:

$$\text{Complexation efficiency} = \frac{F_t - F_A}{F_t} \times 100\% \quad (1)$$

, where F_t and F_A are the fluorescence intensity of Cy3-siRNA before and after centrifugation, respectively.

2.4 Adipose derived mesenchymal stem cell isolation

Adipose derived mesenchymal stem cells (ASCs) were isolated from inguinal fat pads of C57BL/6 mouse (4-8 weeks) as previously described.[14, 38] Briefly, Adipose tissues were harvested, rinsed in sterilized PBS, cut into small pieces and digested with 0.1% collagenase type I. After 2 h of digestion in an incubator, cells were collected by centrifugation at 1200 rpm for 5 min, and resuspended in basal growth medium (DMEM, 10% FBS, 1% P/S). The resuspended cells were seeded onto the tissue culture flasks.

2.5 Cytotoxicity

Cytotoxicity of nanoparticles was evaluated using alamarBlue assay (Invitrogen, Carlsbad, CA). Briefly, ASCs were seeded in 96-well plates at a density of 1×10^4 cells/well. After 24 h incubation, medium was replaced by 100 μL fresh basal growth medium with various concentrations of nanoparticles or complexes. Following 16 h incubation, the medium was replaced with 100 μL of 10% (v/v) alamarBlue solution in basal medium. After 3 h incubation, the fluorescence intensity (F) of alamarBlue was measured at 585 nm with an excitation wavelength of 570 nm. Cells without nanoparticles were set as positive control with 100% viability. As a blank group, the 10% (v/v) alamarBlue solution was added in an empty well without cells and incubated together. The relative cell viability (%) was calculated using the following equation:

$$Relative\ cell\ viability = \frac{F_s - F_b}{F_c - F_b} \times 100\% \quad (2)$$

, where F_s, F_c, and F_b are fluorescence intensity of samples, control group, and blank group, respectively.

2.6. Cellular uptake in 2D monolayer culture

ASCs were seeded onto 8-well chambered glass or 6-well plates for 2D cellular uptake study. When cells were grown to 70 ~ 80% confluence, the basal growth medium was changed to the antibiotic free transfection medium (DMEM, 10% FBS), according to the manufacturer's protocol for siRNA transfection using lipofectamine 2000. The cells were then incubated with the transfection media containing Cy3-siRNA incorporated nanoparticles for 15 h. Although lipofectamine 2000 was efficient at transferring genes into cancer cells or other fast dividing cell lines, it was less effective at transferring siRNA to primary ASCs requiring longer incubation up to 15 h, thus, the same incubation time was used with SA/Chol for a comparison test. Afterwards, the media were aspirated and the cells were washed with PBS to remove any free-floating nanoparticles and Cy3-siRNA. Cells in 8-well chambered glass were fixed with formalin 10% buffered in phosphate (Electron Microscopy Sciences, Hatfield, PA) solution and fluorescence images were observed using an Olympus IX71 microscope (Olympus, Tokyo, Japan). Uptake efficiency (%) was obtained either by counting transfected cells in relation to the total number of cells using ImageJ (n = 6) [39] or by flow cytometry (BD LSRFortessa X-20 SORP, Becton Dickinson, San Jose, CA). Cells in 6-well plate were detached with trypsin (0.05%, Invitrogen), centrifuged for 4 min at 1200 rpm, and resuspended in growth media for flow cytometry analysis. Cy3 was excited using 488-nm laser and detected using longpass dichroic mirror 550LP and bandpass filter 586/15. Cell population of interest was selected from the scatter plot.

2.7 RNA extraction and quantitative real-time polymerase chain reaction (qRT-PCR)

ASCs were seeded onto 12-well plates for 2D gene expression study. When cells were grown to 70 ~ 80% confluence, the basal growth medium was changed to the transfection medium. The cells were then incubated with the transfection media containing noggin-siRNA incorporated nanoparticles for 15 h. Afterwards, the media were aspirated and the

cells were washed with PBS to remove any free-floating nanoparticles and siRNA. After incubation for 3 days and 7 days in an osteogenic medium (DMEM, 10% FBS, 1% P/S, 10 mM β-glycerophosphate, 50 μg/mL L-ascorbic acid, and 100 nM dexamethasone), total RNA was extracted using Trizol reagent and RNeasy Mini kit. 0.5 μg of total RNA was reversely transcribed to cDNA using a cDNA transcription kit (Invitrogen). Quantitative real-time PCR was measured using LightCycler 480 PCR (Indianapolis, IN) with 20 μl SYBR Green reaction system. PCR amplification was performed for 45 cycles. The expression of housekeeping gene (GAPDH) was used to normalize gene expression levels. The following primers were used in this experiment — *GAPDH*: AGGTCGGTGTGAACGGATTTG (forward), TGTAGACCATGTAGTTGAGGTCA (reverse); *Noggin*: GCCAGCACTATCTACACATCC (forward), GCGTCTCGTTCAGATCCTTCTC (reverse); *Alkaline phosphatase (ALP)*: GTTGCCAAGCTGGGAAGAACAC (forward), CCCACCCCGCTATTCCAAAC (reverse); *Runt-related transcription factor 2* (*Runx2*): CGGTCTCCTTCCAGGATGGT (forward), GCTTCCGTCAGCGTCAACA (reverse); *Osteocalcin (OCN)*: GGGAGACAACAGGGAGGAAAC (forward), CAGGCTTCCTGCCAGTACCT (reverse).

2.7 3D hydrogel preparation and cell culture

Photocrosslinkable methacrylated glycol chitosan (MeGC) was prepared as previously described [40]. Mix ASCs at a density of 2×10^6 cells/mL and nanoparticle-siRNA complexes (final concentration of 100 nM for siRNA) in MeGC solution (final concentration of 2% w/v). The hydrogel was formed by exposing 40 μL of the suspension to visible blue-light (400 - 500 nm, 500 - 600 mW/cm^2, Bisco Inc., Schaumburg, IL) in the presence of a photoinitiator, riboflavin (final concentration 6 μM). Prepared hydrogels were incubated first in 1 mL of transfection media for 15 h, and osteogenic medium was used to replace the transfection medium.

2.8 Alkaline phosphatase and Alizarin red S staining

At a predetermined time point, gels were fixed in formalin 10% buffered in phosphate for 20 min, washed with PBS, and incubated in a solution consisting of NBT and BCIP stock solutions in ALP buffer (100 mM Tris, 50 mM MgCl2, 100 mM NaCl, pH 8.5) for 2 h. The stained samples were observed with the Olympus SZX16 Stereomicroscope (Olympus, Tokyo, Japan). ALP expression appeared in blue.

Gels were fixed in formalin 10% buffered in phosphate for 20 min, washed with PBS, and incubated in 2% Alizarin red S solution for 5 min. Then, the gels were washed with PBS under gentle shaking for 16 h, and the PBS was changed at least three times. The stained samples were then observed with the Olympus SZX16 Stereomicroscope. Calcium deposition exhibited in red.

2.9 Calvarial defect model

The surgical procedures were performed in accordance with the guidelines of the Chancellor's Animal Research Committee at the University of California, Los Angeles. Calvaria of male CD-1 nude mice (8-12 weeks old) were exposed to a trephine drill under constant irrigation and 3-mm full-thickness craniotomy defects were created in the left side

of parietal bone with care to avoid injury to the underlying dura mater. Each defect was syringed with sterile saline solution to remove bone debris and then implanted with MeGC hydrogels containing nanoparticles-siRNA complexes and cells or left without any treatment. After surgery, all animals were allowed to recover on a warm sheet and then transferred to the vivarium for postoperative care. To get operative treatment, all animals received analgesia with subcutaneous injections of buprenorphine with a concentration of 0.1 mg/kg for 3 days. To prevent potential infection, all animals received drinking water including trimethoprim-sulfamethoxazole for 7 days.

2.10 Three-dimensional micro-computerized tomography (μCT) scanning

After 6 weeks post-implantation, animals were sacrificed and calvarial tissues were harvested for analysis. The extracted calvarial tissues were fixed in 4% formaldehyde at room temperature with gentle shaking. After 48 h, the fixed samples were rinsed with PBS and stored in 70% ethanol at 4 °C before imaging using the high–resolution μCT (SkyScan 1172; SkyScan, Kontich, Belgium) with 57 kVp, 184 μA, 0.5 mm aluminum filtration and 10 μm resolution. Visualization and reconstruction of the data were obtained using Dolphin 3D software (Dolphin Imaging & Management Solutions, Chatsworth, CA). New bone surface area was measured using Image J software (NIH, Bethesda, Maryland), and normalized to the original defect surface area (3 mm in diameter).

2.11 Histological evaluation

The fixed tissues were decalcified under 10% EDTA solution under gentle shaking for 1 week. The EDTA solution was changed once at day 3. Decalcified samples were embedded in paraffin and cut into sections of 5 μm thickness. The tissue sections were deparaffinized and stained with hematoxyline and eosin (H&E). Masson-Goldner trichrome staining was also performed to detect new bone formation. The light green solution was used to stain bone tissue. The green color indicated new or mature bone, observed using an Olympus IX71 microscope. The distances between the gaps were measured with ImageJ, and normalized to the blank group. Immunohistochemistry was performed on additional sections for detecting noggin expression at week 6. The deparaffinized sections were treated using citric acid antigen retrieval, incubated with the primary antibodies against noggin (Santa Cruz Biotechnology Inc., CA) and antibody was detected using HRP/DAB detection kit (Abcam, MA), as per manufacturer's instructions.

2.12 Statistical analysis

Three independent experiments, unless otherwise stated, were carried out and the error bars in all figures represent standard deviation. Statistical analysis was performed using the analysis of variances (ANOVA) followed by Tukey's post hoc test. A value of $p < 0.05$ was considered statistically significant.

3. Results and discussion

3.1 Cytotoxicity

Although the positive charge of cationic liposomes can facilitate intracellular uptake, it also associates with cytotoxicity [41-43] resulted from the generation of reactive oxygen

intermediates, toxic oxidative bursts, and a disruption of cellular and sub-cellular membrane functions. The cytotoxicity of SA/Chol Sterosomes and their complexes with siRNA was evaluated in primarily harvested ASCs at various particle concentrations using an alamarBlue assay in comparison with commercially available lipofectamine 2000 (Fig. 1). Lipofectamine 2000 has been used successfully to transfect synthetic siRNA into mammalian cells [22]. SA/Chol and lipofectamine 2000 vesicles showed a high level of cell viability up to 5 μg/mL (Fig. 1A). Further increasing the particle concentration above 5 μg/mL led to lower cell viability. There was no significant difference in cell viability between SA/Chol and lipofectamine 2000 vesicles. No significant cytotoxicity was observed for both SA/Chol Sterosomes and lipofectamine 2000 vesicles when they were complexed with siRNA up to 10 μg/mL particles and 200 nM siRNA (Fig. 1B). The negative charges that siRNA carries could partially neutralize the positive charges possessed by the particles, leading to less toxic complexes compared to empty particles. SA/Chol Sterosomes were used at 5 μg/mL in the following experiments to ensure great cell viability and also to directly compare with lipofectamine 2000.

3.2 Characterization and stability of SA/Chol vesicles and SA/Chol-siRNA complexes

Stability and zeta potential of SA/Chol LUVs and their complexes with siRNA were further characterized. The hydrodynamic diameters were around 110 and 140 nm for SA/Chol vesicles and SA/Chol-siRNA complexes at 37 °C, respectively and remained constant during incubation up to 14 days (Fig. 2A), with a low polydispersity index (PDI < 0.4) (Fig. 2B). The observed increase in the hydrodynamic size after the complexation may be due to the hydrophilicity and crown layer of siRNA molecules created on top of the Sterosomes. The storage stability of SA/Chol LUVs was also studied by incubating them at lower temperatures of 4 and 25 °C for 14 days. The hydrodynamic diameters of SA/Chol vesicles were increased from 100 to 140 nm as temperature decreased from 25 to 4 °C (Fig. S1A), with a low PDI (Fig. S1B). Temperature can have significant effects on the elasticity of bilayer membranes, resulting in a significant change in vesicle size [44]. Given that no phase transition was observed between 25 and 80 °C for SA/Chol equimolar mixture [35], the observed significant change in vesicle diameter may be due to the decreased mobility of the SA and Chol molecules in the bilayer as temperature decreased from 25 to 4 °C, thereby affecting on the elasticity of the membranes and final vesicle size. The hydrodynamic diameters between 25 and 37 °C were very close, 100 and 110 nm. The liposomal surface charge density can be conveniently investigated by microelectrophoresis and characterized by the zeta potential. The zeta potential of Sterosomes crafted from equimolar SA/Chol mixtures was 55 ± 2 mV at pH 7.4, indicating that the suspension is very stable [45]. With increasing the concentration of siRNA, the zeta potential of the complexes decreased dramatically (Fig. 2C). With 200 nM siRNA, the zeta potential decreased to ~15 mV, suggesting that this colloidal system is unstable and would eventually aggregate. For 100 nM siRNA, the zeta potential was about 33 mV, suggesting an intermediate stable system. We therefore monitored the zeta potential of this complex during incubation at 37 °C up to 14 days. The zeta potential of the complexes (100 nM siRNA) was not significantly changed during the incubation, indicating that the system was stable at least for 2 weeks (Fig. 2D). The presence of charge on the surface of SA/Chol vesicles favors the electrostatic repulsion among them, preventing their aggregation and flocculation. We varied the external pH of an

equimolar SA/Chol Sterosomes suspension initially prepared at pH 7.4 and measured the hydrodynamic diameter (Figure S1C). No significant change in vesicle size was observed below pH 8. In contrast, increasing the external pH above 8 led to significant increase in vesicle size. The size measurement was not possible above pH 10 by the zetasizer because of the high polydispersity. The observed increase in the vesicle size with the pH increase is likely due to the progressive deprotonation of the amine groups in the vesicles that may result in the loss of surface charge and thereby complete aggregation of the colloidal system. Typically, conventional liposomes were made of phospholipid molecules, which suffer from hydrolysis and oxidation, leading to limited shelf life [46]. However, SA/Chol Sterosomes were stable over a large pH and temperature range. The SA/Chol Sterosomes and SA/Chol-siRNA complexes are stable enough to be readily stored at room temperature or 37 °C.

3.3 Complexation and uptake efficiency

The complexation efficiency of lipofectamine 2000 and SA/Chol vesicles with 100 nM siRNA was 69 ± 2% and 84 ± 3%, respectively. Typically, higher positive surface charge density leads to higher uptake efficiency and more stable system. One of the essential properties of gene delivery vehicles is the uptake efficiency. The uptake efficiency of lipoplexes and SA/Chol-siRNA complexes was characterized for freshly prepared and incubated samples (Table 1 and Fig. 3). The high uptake efficiencies of 93% and 96% were observed for lipofectamine 2000 and SA/Chol particles, respectively. After 14 days incubation at 37 °C, more than 60% uptake efficiency was observed for SA/Chol-siRNA complexes, while very little uptake was detected for lipoplexes. We have also examined the uptake efficiency of SA/Chol vesicles under challenging conditions, such as incubating at various temperatures, with organic solvent for 14 days, or extreme acidic pH for 1 h. All of the vesicles showed great uptake ability, ~97%, comparable to freshly prepared lipofectamine 2000 and SA/Chol vesicles (Table S1 and Fig. S2). SA has been previously used to provide a positive charge to conventional phospholipid liposomes [47, 48], in order to enhance the stability and reduce the permeability of the encapsulated drugs. The new SA/Chol vesicles exhibit distinct properties: stable systems that can be stored at room temperature, increased positive surface charge, high complexation efficiency, high uptake efficiency even after incubation, which make them promising siRNA delivery nanocarriers.

3.4 Gene expressions

Noggin gene expression after transfection with lipofectamine 2000 and SA/Chol vesicles was evaluated with qRT-PCR. Significant noggin suppression was observed (Fig. 4). More than 45% of noggin was knocked down by siRNA delivered by SA/Chol vesicles compared to the blank group, while only approximately 25% for the lipofectamine 2000 delivery group. Under the same conditions, the gene knockdown efficiency of noggin siRNA delivered by SA/Chol Sterosomes is significantly higher than the commercially available lipofectamine 2000. Approximately 40-70% noggin knockdown was observed in ASCs transduced with noggin-targeted shRNA lentiviral particles in our previous study [13]. Less than 20% noggin knockdown has been reported using PEI/siRNA complexes to transduce human MSCs [49].

In addition, effects of noggin suppression on osteogenic differentiation of ASCs on 2D culture plates were assessed by the gene expression of *ALP*, an early osteogenic marker, and *Runx2*, one of the most specific osteogenic differentiation markers in earlier stage and *OCN*, a late osteogenic marker (Fig. 5). Noggin suppression increased *ALP* and *Runx2* expression by ~1.3 fold for both lipofectamine 2000 and SA/Chol groups comparing to corresponding control groups. For the late marker *OCN* on day 7, 1.4 and 1.6 fold upregulation was observed for lipofectamine 2000 and SA/Chol groups, respectively. Similar upregulation results on the expression of *Runx2* and *OCN* were reported by using noggin shRNA lentiviral particles [13]. It was shown that on day 14, ~1.4 and ~1.7 fold upregulation was observed for *Runx2* and *OCN* after noggin shRNA lentiviral transduction. Although the expression level of noggin in SA/Chol group was significantly lower than that detected in lipofectamine group (Fig. 4), there was no statistically significant difference between the groups with respect to osteogenic gene expressions. Our SA/Chol Sterosomes are comparable to lentiviral particles and lipofectamine 2000 on those gene marker expressions.

3.5 In vitro 3D model

MeGC hydrogels were utilized to provide a 3D *in vitro* environment to further evaluate the differentiation of ASCs transfected by noggin siRNA delivered using lipofectamine 2000 and SA/Chol Sterosomes. *In situ* forming 3D hydrogels have been attractive for tissue engineering applications owing to their injectability and capacity to gel to take the shape of defects and the capacity to encapsulate cells with high viability [50, 51]. We previously demonstrated that the injectable hydrogel system composed of visible blue-light inducible chitosan and riboflavin initiator supported proliferation and osteo- or chondrogenic differentiation of encapsulated MSCs [40, 52, 53]. In light of this, we examined the osteogenic differentiation of ASCs transfected by siRNA delivered by lipofectamine 2000 or SA/Chol Sterosomes encapsulated in the MeGC hydrogel system [40]. ALP and Alizarin Red S staining were performed after siRNA transfection to examine the ALP expression and calcium deposition. A blank gel without cells was formed to be the negative assay control, while all the other groups contained ASCs.

As shown in Fig. 6, the noggin siRNA delivered by lipofectaimine 2000 and SA/Chol vesicles induced the strongest ALP expression. ALP expression of all groups increased over time since the hydrogels were cultured in osteogenic media. Because ALP is an early marker for osteogenesis and the expression of ALP does not necessarily induce osteogenic differentiation, it is essential to evaluate additional osteogenic differentiation indicators. Mineralization is well known to be the ultimate stage of osteogenic differentiation; the calcium deposition was examined by Alizarin red S staining. Fig. 7 revealed increased extracellular matrix mineralization for noggin siRNA groups compared with control siRNA groups, suggesting that noggin suppression significantly enhanced osteogenic differentiation of cells. The control siRNA groups showed stronger staining for ALP and Alizarin red than the cell alone groups. Random sequenced control siRNA used in these experiments may have non-specific silencing effects resulting in the expression on ALP and mineralization. Further study will be performed to titrate siRNA concentrations to minimize the non-specific effects. Altogether, the *in vitro* data are consistent and indicate SA/Chol Sterosomes are effective noggin siRNA nanocarriers to enhance osteogenic differentiation.

3.6 In vivo calvarial defect model

We examined the possibility of translating the 3D systems to *in vivo* environment. We took a further step with mouse calvarial defects model to evaluate the *in vivo* bone repair effects six weeks post surgery. 3 mm critical size calvarial defects were prepared for each group. The blank group was left empty without any treatment after creating the defect. All the other groups were treated with *in situ* forming MeGC hydrogels encapsulating cells and siRNA loaded nanoparticles. The representative microCT images (Fig. 8A) show that the size of the defects treated with ASCs (CtrRNA groups) were smaller than the blank control group. The observed increased bone healing in the control siRNA groups may be due to osteogenic differentiation of engrafted ASCs with hydrogels. Both of the groups treated with noggin siRNA delivered by lipofectamine 2000 and SA/Chol vesicles showed the most bone healing compared to other control groups. The relative new bone surface area was calculated to quantitatively analyze the microCT images (Fig. 8B). The original defect area (3 mm in diameter) was used to normalize the results. Almost no healing in the blank group was observed after 6 weeks compared to its original size. Defects treated with noggin siRNA delivered by lipofectamine 2000 and SA/Chol vesicles were filled ~15% and ~20% by new bone, respectively. In contrast, defects treated with control siRNA showed a minimal healing (~5%) after 6 weeks.

The new bone formation was further characterized with histological analysis (Fig. 9A). H&E staining showed that the edges of defects treated with noggin siRNA were filled with bone formation at 6 weeks. Masson-Goldner trichrome staining showed formation of osteoid matrix on the edges of defects treated with noggin siRNA, while control groups only exhibited fibrous-like tissue with minimal bone formation. The gap of the defects was quantified with ImageJ by measuring the distance between advancing edges (Fig. 9B). For SA/Chol-nogRNA and lipo-nogRNA, the distances of defects decreased by 33% and 27% compared to blank group, respectively. Furthermore, we evaluated expression of noggin after 6 weeks post-implantation by immunohistochemical staining for noggin. Noggin staining was reduced in the nogRNA groups for both SA/Chol and lipofectaime 2000 compared to their corresponding control siRNA groups. Noggin was detected minimally in SA/Chol-nogRNA group, suggesting high gene knockdown efficiency of SA/Chol Sterosomes in vivo.

In this study, knockdown of noggin expression executed by lipid based nanoparticle delivery demonstrated enhanced both osteogenesis *in vitro* and bone formation *in vivo*. Based on all of the above results, we believe that cationic Sterosome formulated with SA/Chol is a very efficient gene delivery vector. Although cholesterol can affect osteoblastic differentiation [37], the in vivo bone healing was not very satisfactory. Since the composition is very versatile, it would be a good idea to craft Steromsomes with more osteoinductive cholesterol derivatives, such as oxysterols [54, 55]. The defects were not fully repaired during the time course of six weeks. It would be of interest to simultaneously deliver other osteoinductive stimulates and explore synergistic effects with noggin siRNA on bone regeneration. Moreover, the vector biodistribution and toxicological profiling is critical for the future clinical translation and further study will be performed to assess this.

4. Conclusion

We investigated the ability of the new cationic Sterosomes consisting of equimolar monoalkylated primary amine (SA) and Chol to deliver siRNA for efficient gene knockdown and osteogenesis. SA/Chol Sterosomes demonstrated significantly increased particle stability and gene knockdown efficiency with minimal toxicity compared with commercially available lipofectamine 2000. Moreover, suppression of noggin expression via this Sterosome vehicle enhanced the osteogenesis of ASCs *in vitro* and promoted bone regeneration *in vivo*. These results suggest that our Sterosome system has a great potential as a non-viral gene delivery modality and may provide new opportunities for gene therapies.

Supplementary Material

Refer to Web version on PubMed Central for supplementary material.

Acknowledgements

This work was supported by the National Institutes of Health grants R01 AR060213 and R21 DE021819, the International Association for Dental Research, and the Academy of Osseointegration. Flow cytometry was performed in the UCLA Jonsson Comprehensive Cancer Center (JCCC) and Center for AIDS Research Flow Cytometry Core Facility that is supported by National Institutes of Health awards P30 CA016042 and 5P30 AI028697, and by the JCCC, the UCLA AIDS Institute, the David Geffen School of Medicine at UCLA, the UCLA Chancellor's Office, and the UCLA Vice Chancellor's Office of Research.

References

[1]. Pannier AK, Shea LD. Controlled release systems for DNA delivery. Mol. Ther. 2004; 10:19–26. [PubMed: 15233938]

[2]. Flotte TR. Gene therapy: the first two decades and the current state-of-the-art. J. Cell. Physiol. 2007; 213:301–305. [PubMed: 17577203]

[3]. Niidome T, Huang L. Gene therapy progress and prospects: nonviral vectors. Gene Ther. 2002; 9:1647–1652. [PubMed: 12457277]

[4]. Fire A, Xu SQ, Montgomery MK, Kostas SA, Driver SE, Mello CC. Potent and specific genetic interference by double-stranded RNA in Caenorhabditis elegans. Nature. 1998; 391:806–811. [PubMed: 9486653]

[5]. Oh YK, Park TG. siRNA delivery systems for cancer treatment. Adv. Drug Deliv. Rev. 2009; 61:850–862. [PubMed: 19422869]

[6]. Kim DH, Rossi JJ. Strategies for silencing human disease using RNA interference. Nat. Rev. Genet. 2007; 8:173–184. [PubMed: 17304245]

[7]. Jung JJ, Solanki A, Memoli KA, Kamei K, Kim H, Drahl MA, Williams LJ, Tseng HR, Lee K. Selective Inhibition of Human Brain Tumor Cells through Multifunctional Quantum-Dot-Based siRNA Delivery. Angew. Chem. 2010; 49:103–107. [PubMed: 19950159]

[8]. Park HJ, Shin J, Kim J, Cho SW. Nonviral delivery for reprogramming to pluripotency and differentiation. Arch. Pharm. Res. 2014; 37:107–119. [PubMed: 24222505]

[9]. Yau WWY, Rujitanaroj PO, Lam L, Chew SY. Directing stem cell fate by controlled RNA interference. Biomaterials. 2012; 33:2608–2628. [PubMed: 22209557]

[10]. Wan DC, Pomerantz JH, Brunet LJ, Kim JB, Chou YF, Wu BM, Harland R, Blau HM, Longaker MT. Noggin suppression enhances in vitro osteogenesis and accelerates in vivo bone formation. J. Biol. Chem. 2007; 282:26450–26459. [PubMed: 17609215]

[11]. Gazzerro E, Gangji V, Canalis E. Bone morphogenetic proteins induce the expression of noggin, which limits their activity in cultured rat osteoblasts. J. Clin. Investig. 1998; 102:2106–2114. [PubMed: 9854046]

[12]. Gazzerro E, Du Z, Devlin RD, Rydziel S, Priest L, Economides A, Canalis E. Noggin arrests stromal cell differentiation in vitro. Bone. 2003; 32:111–119. [PubMed: 12633782]

[13]. Fan J, Park H, Tan S, Lee M. Enhanced Osteogenesis of Adipose Derived Stem Cells with Noggin Suppression and Delivery of BMP-2. Plos One. 2013; 8:e72474. [PubMed: 23977305]

[14]. Fan J, Park H, Lee M, Bezouglaia O, Kim J, Aghaloo T, Lee M. Adipose derived stem cells and BMP-2 delivery in chitosan-based 3D constructs to enhance bone regeneration in a rat mandibular defect model. Tissue Eng. Part A. 2014; 20:2169–2179. [PubMed: 24524819]

[15]. Thomas CE, Ehrhardt A, Kay MA. Progress and problems with the use of viral vectors for gene therapy. Nat. Rev. Genet. 2003; 4:346–358. [PubMed: 12728277]

[16]. Park HJ, Yang F, Cho SW. Nonviral delivery of genetic medicine for therapeutic angiogenesis. Adv. Drug Deliv. Rev. 2012; 64:40–52. [PubMed: 21971337]

[17]. Liu T, Tang A, Zhang G, Chen Y, Zhang J, Peng S, Cai Z. Calcium phosphate nanoparticles as a novel nonviral vector for efficient transfection of DNA in cancer gene therapy. Cancer Biother. Radiopharm. 2005; 20:141–149. [PubMed: 15869447]

[18]. Bessis N, GarciaCozar FJ, Boissier MC. Immune responses to gene therapy vectors: influence on vector function and effector mechanisms. Gene Ther. 2004; 11:S10–S17. [PubMed: 15454952]

[19]. Waehler R, Russell SJ, Curiel DT. Engineering targeted viral vectors for gene therapy. Nat. Rev. Genet. 2007; 8:573–587. [PubMed: 17607305]

[20]. Bouard D, Alazard-Dany N, Cosset FL. Viral vectors: from virology to transgene expression. Br. J. Pharmacol. 2009; 157:153–165. [PubMed: 18776913]

[21]. Baum C, Kustikova O, Modlich U, Li ZX, Fehse B. Mutagenesis and oncogenesis by chromosomal insertion of gene transfer vectors. Hum. Gene. Ther. 2006; 17:253–263. [PubMed: 16544975]

[22]. Elbashir SM, Harborth J, Lendeckel W, Yalcin A, Weber K, Tuschl T. Duplexes of 21-nucleotide RNAs mediate RNA interference in cultured mammalian cells. Nature. 2001; 411:494–498. [PubMed: 11373684]

[23]. Bumcrot D, Manoharan M, Koteliansky V, Sah DW. RNAi therapeutics: a potential new class of pharmaceutical drugs. Nat. Chem. Biol. 2006; 2:711–719. [PubMed: 17108989]

[24]. Mellott AJ, Forrest ML, Detamore MS. Physical non-viral gene delivery methods for tissue engineering. Ann. Biomed. Eng. 2013; 41:446–468. [PubMed: 23099792]

[25]. Gresch O, Engel FB, Nesic D, Tran TT, England HM, Hickman ES, Korner I, Gan L, Chen S, Castro-Obregon S, Hammermann R, Wolf J, Muller-Hartmann H, Nix M, Siebenkotten G, Kraus G, Lun K. New non-viral method for gene transfer into primary cells. Methods. 2004; 33:151–163. [PubMed: 15121170]

[26]. Lin QY, Chen J, Zhang ZH, Zheng G. Lipid-based nanoparticles in the systemic delivery of siRNA. Nanomed. 2014; 9:105–120.

[27]. Torchilin VP. Recent advances with liposomes as pharmaceutical carriers. Nat. Rev. Drug Discov. 2005; 4:145–160. [PubMed: 15688077]

[28]. Papakostas D, Rancan F, Sterry W, Blume-Peytavi U, Vogt A. Nanoparticles in dermatology. Arch. Dermatol. Res. 2011; 303:533–550. [PubMed: 21837474]

[29]. Fathi M, Mozafari MR, Mohebbi M. Nanoencapsulation of food ingredients using lipid based delivery systems. Trends Food Sci. Technol. 2012; 23:13–27.

[30]. Barani H, Montazer M. A review on applications of liposomes in textile processing. J. Liposome Res. 2008; 18:249–262. [PubMed: 18770074]

[31]. Xu Y, Szoka FC. Mechanism of DNA release from cationic liposome/DNA complexes used in cell transfection. Biochemistry. 1996; 35:5616–5623. [PubMed: 8639519]

[32]. Zelphati O, Szoka FC. Intracellular distribution and mechanism of delivery of oligonucleotides mediated by cationic lipids. Pharm. Res. 1996; 13:1367–1372. [PubMed: 8893276]

[33]. Hong K, Zheng W, Baker A, Papahadjopoulos D. Stabilization of cationic liposome-plasmid DNA complexes by polyamines and poly(ethylene glycol)-phospholipid conjugates for efficient in vivo gene delivery. FEBS Lett. 1997; 400:233–237. [PubMed: 9001404]

[34]. Cui ZK, Lafleur M. Lamellar self-assemblies of single-chain amphiphiles and sterols and their derived liposomes: Distinct compositions and distinct properties. Colloid Surf. B-Biointerfaces. 2014; 114:177–185.

[35]. Cui Z-K, Bouisse A, Cottenye N, Lafleur M. Formation of pH-sensitive cationic liposomes from a binary mixture of monoalkylated primary amine and cholesterol. Langmuir. 2012; 28:13668–13674. [PubMed: 22931455]

[36]. Son KK, Patel DH, Tkach D, Park A. Cationic liposome and plasmid DNA complexes formed in serum-free medium under optimum transfection condition are negatively charged. Biochim. Biophys. Acta-Biomembr. 2000; 1466:11–15.

[37]. Li HF, Guo HJ, Li H. Cholesterol loading affects osteoblastic differentiation in mouse mesenchymal stem cells. Steroids. 2013; 78:426–433. [PubMed: 23395977]

[38]. Estes BT, Diekman BO, Gimble JM, Guilak F. Isolation of adipose-derived stem cells and their induction to a chondrogenic phenotype. Nat. Protoc. 2010; 5:1294–1311. [PubMed: 20595958]

[39]. Luhmann T, Rimann M, Bittermann AG, Hall H. Cellular uptake and intracellular pathways of PLL-g-PEG-DNA nanoparticles. Bioconjug. Chem. 2008; 19:1907–1916. [PubMed: 18717536]

[40]. Hu J, Hou Y, Park H, Choi B, Hou S, Chung A, Lee M. Visible light crosslinkable chitosan hydrogels for tissue engineering. Acta Biomater. 2012; 8:1730–1738. [PubMed: 22330279]

[41]. Campbell PI. Toxicity of some charged lipids used in liposome preparations. Cytobios. 1983; 37:21–26. [PubMed: 6851664]

[42]. Dokka S, Toledo D, Shi XG, Castranova V, Rojanasakul Y. Oxygen radical-mediated pulmonary toxicity induced by some cationic liposomes. Pharm. Res. 2000; 17:521–525. [PubMed: 10888302]

[43]. Romoren K, Thu BJ, Bols NC, Evensen O. Transfection efficiency and cytotoxicity of cationic liposomes in salmonid cell lines of hepatocyte and macrophage origin. Biochim. Biophys. Acta-Biomembr. 2004; 1663:127–134.

[44]. Zook JM, Vreeland WN. Effects of temperature, acyl chain length, and flow-rate ratio on liposome formation and size in a microfluidic hydrodynamic focusing device. Soft Matter. 2010; 6:1352–1360.

[45]. Muller RH, Jacobs C, Kayser O. Nanosuspensions as particulate drug formulations in therapy rationale for development and what we can expect for the future. Adv. Drug Deliv. Rev. 2001; 47:3–19. [PubMed: 11251242]

[46]. Grit M, Crommelin JA. Chemical stability of liposomes: Implications for their physical stability. Chem. Phys. Lipids. 1993; 64:3–18. [PubMed: 8242840]

[47]. Gonzalez-Rodriguez ML, Rabasco AM. Charged liposomes as carriers to enhance the permeation through the skin. Expert Opin. Drug Deliv. 2011; 8:857–871. [PubMed: 21557706]

[48]. Webb MS, Wheeler JJ, Bally MB, Mayer LD. The cationic lipid stearylamine reduces the permeability of the cationic drugs verapamil and prochlorperazine to lipid bilayers - implications for drug-delivery. Biochim. Biophys. Acta-Biomembr. 1995; 1238:147–155.

[49]. Nguyen MK, Jeon O, Krebs MD, Schapira D, Alsberg E. Sustained localized presentation of RNA interfering molecules from in situ forming hydrogels to guide stem cell osteogenic differentiation. Biomaterials. 2014; 35:6278–6286. [PubMed: 24831973]

[50]. Nguyen MK, Lee DS. Injectable biodegradable hydrogels. Macromol. Biosci. 2010; 10:563–579. [PubMed: 20196065]

[51]. Slaughter BV, Khurshid SS, Fisher OZ, Khademhosseini A, Peppas NA. Hydrogels in Regenerative Medicine. Adv. Mater. 2009; 21:3307–3329. [PubMed: 20882499]

[52]. Park H, Choi B, Hu J, Lee M. Injectable chitosan hyaluronic acid hydrogels for cartilage tissue engineering. Acta Biomater. 2013; 9:4779–4786. [PubMed: 22935326]

[53]. Arakawa C, Ng R, Tan S, Kim S, Wu B, Lee M. Photopolymerizable chitosan-collagen hydrogels for bone tissue engineering. J. Tissue Eng. Regen. Med. 2014

[54]. Amantea CM, Kim WK, Meliton V, Tetradis S, Parhami F. Oxysterol-induced osteogenic differentiation of marrow stromal cells is regulated by Dkk-1 inhibitable and PI3-Kinase mediated signaling. J. Cell. Biochem. 2008; 105:424–436. [PubMed: 18613030]

[55]. Lee JS, Yang JH, Hong JY, Jung UW, Yang HC, Lee IS, Choi SH. Early bone healing onto implant surface treated by fibronectin/oxysterol for cell adhesion/osteogenic differentiation: in

vivo experimental study in dogs. J. Periodontal Implant Sci. 2014; 44:242–250. [PubMed: 25368813]

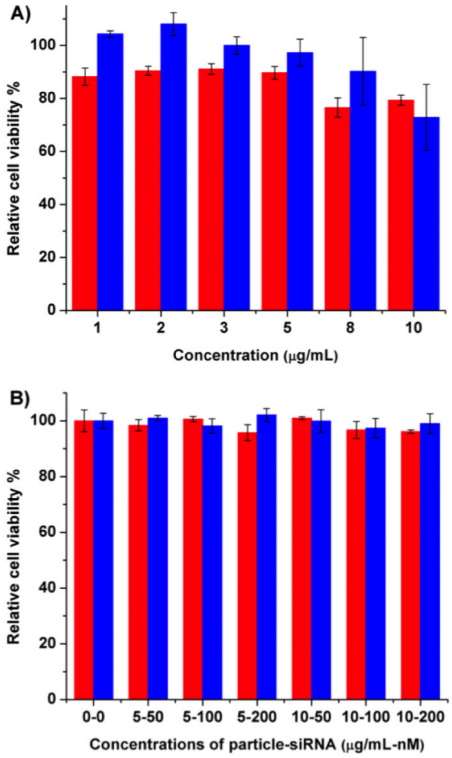

Figure 1.

Cytotoxicity of various concentrations of (A) SA/Chol (blue) and lipofectamine 2000 (red) vesicles; and (B) SA/Chol-siRNA complexes (blue) and lipofectamine 2000-siRNA complexes; evaluated via relative cell viability. (n = 3)

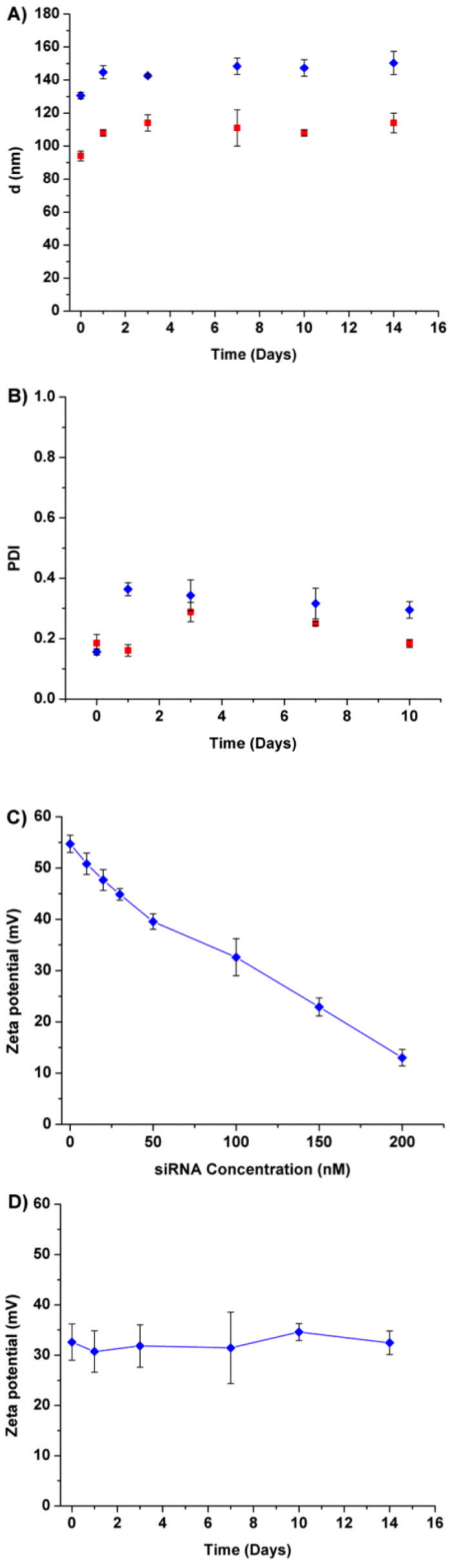

Figure 2.

Characteristics of SA/Chol vesicles and SA/Chol-siRNA complexes. Hydrodynamic size (A) and PDI (B) of SA/Chol vesicles (■) and SA/Chol-siRNA complexes (◆) incubated at 37 °C for 2 weeks; (C) Zeta potential of SA/Chol vesicles and siRNA complexes at a function of various siRNA concentrations; (D) Zeta potential of SA/Chol-siRNA complexes incubated at 37 °C for 2 weeks. (n = 3)

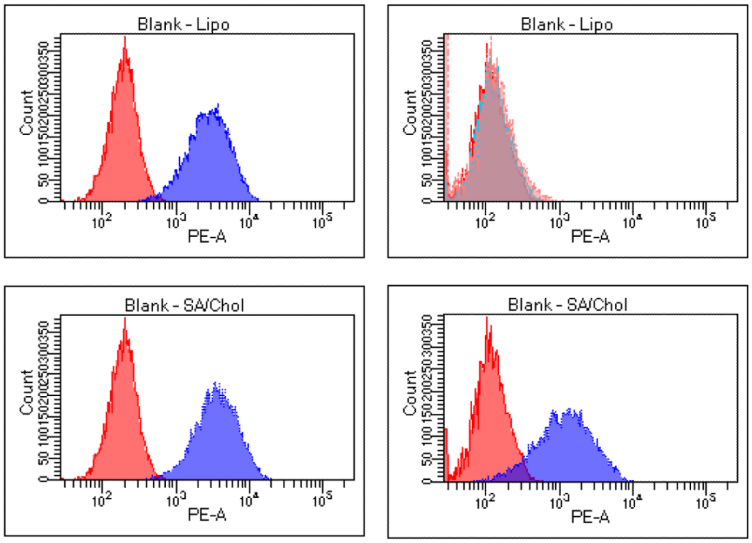

Figure 3.

Flow cytometry. Histogram overlays of non-transfected (blank, red) and transfected (Lipo or SA/Chol, blue) cells. Lipofectamine 2000-siRNA and SA/Chol-siRNA complexes freshly prepared (left panel) and kept at 37 °C for 14 days (right panel). (n = 3)

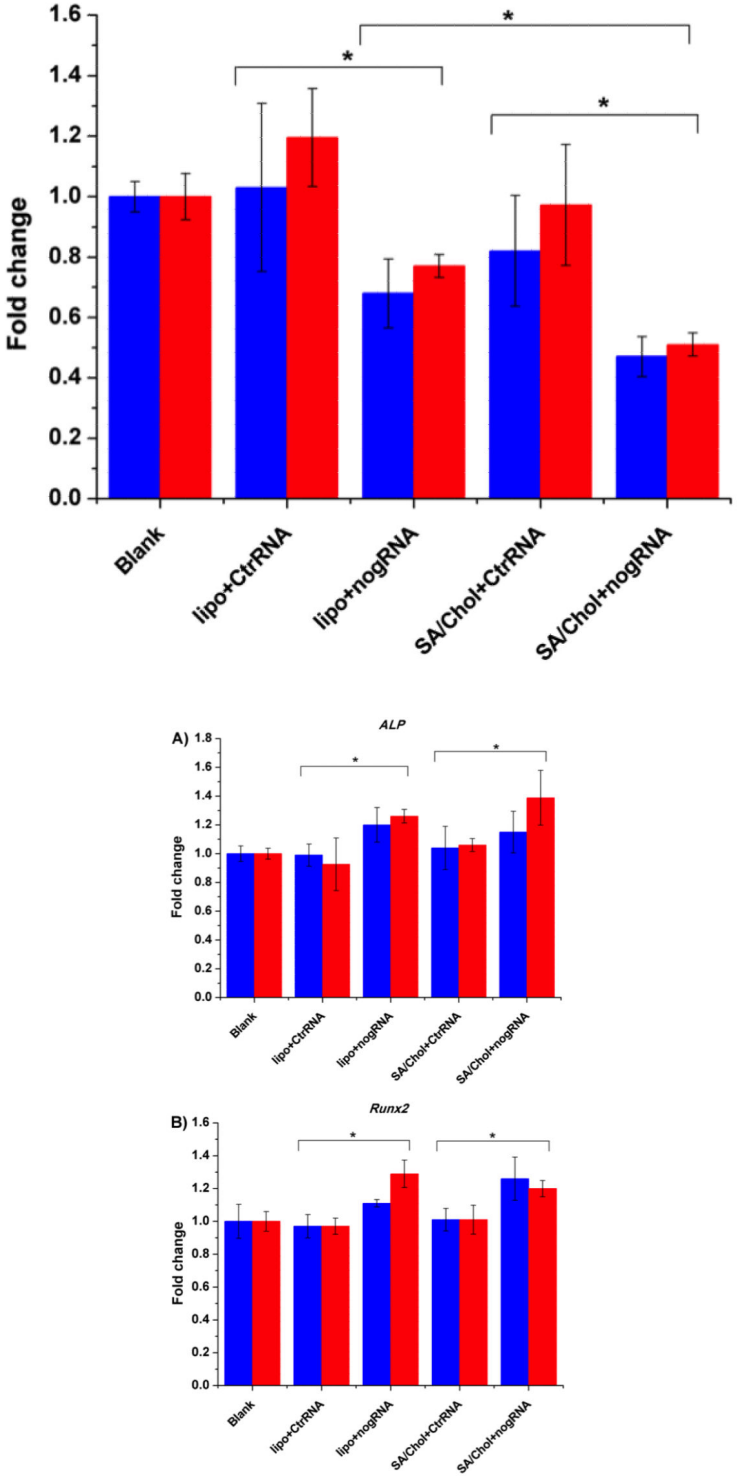

Figure 4.

Expression of noggin gene in ASCs transfected with lipofectamine 2000 and SA/Chol vesicles (n = 5), day 3 (blue) and 7 (red). Significantly lower noggin expression was observed (*$p < 0.05$).

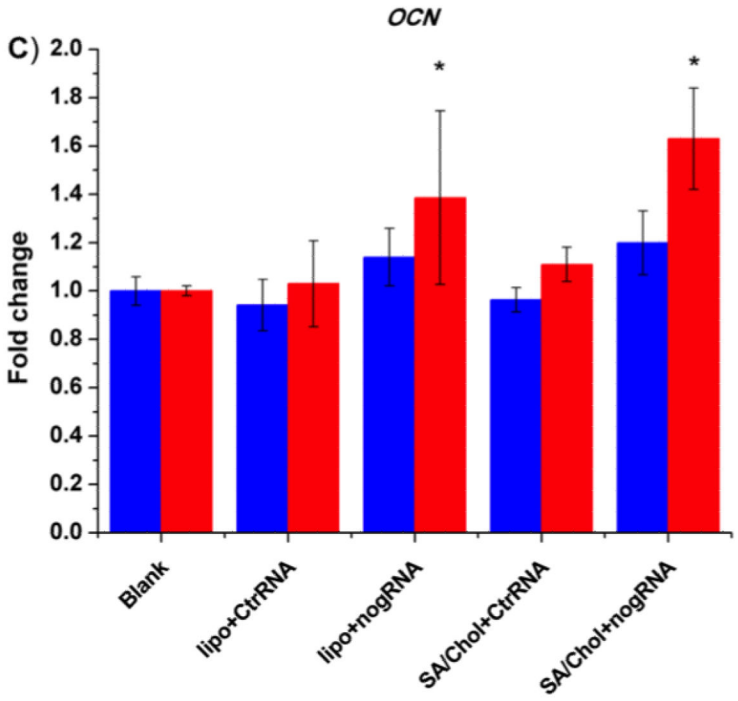

Figure 5.

Osteogenic gene expression of ASCs in monolayer culture. Osteogenic gene markers including *ALP* (A), *Runx2* (B), and *OCN* (C), were evaluated for day 3 (blue) and 7 (red), (n = 5, *p < 0.05, compared to its corresponding control group).

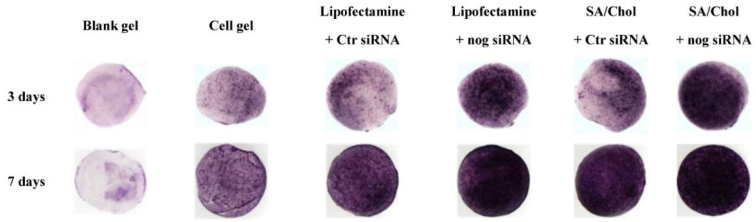

Figure 6.
Alkaline phosphatase (ALP) expression of ASCs in hydrogels.

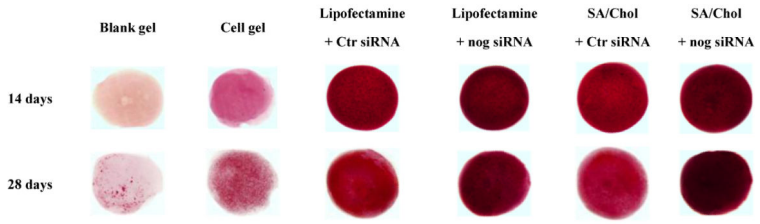

Figure 7.
Mineralization in hydrogels stained with Alizarin red S.

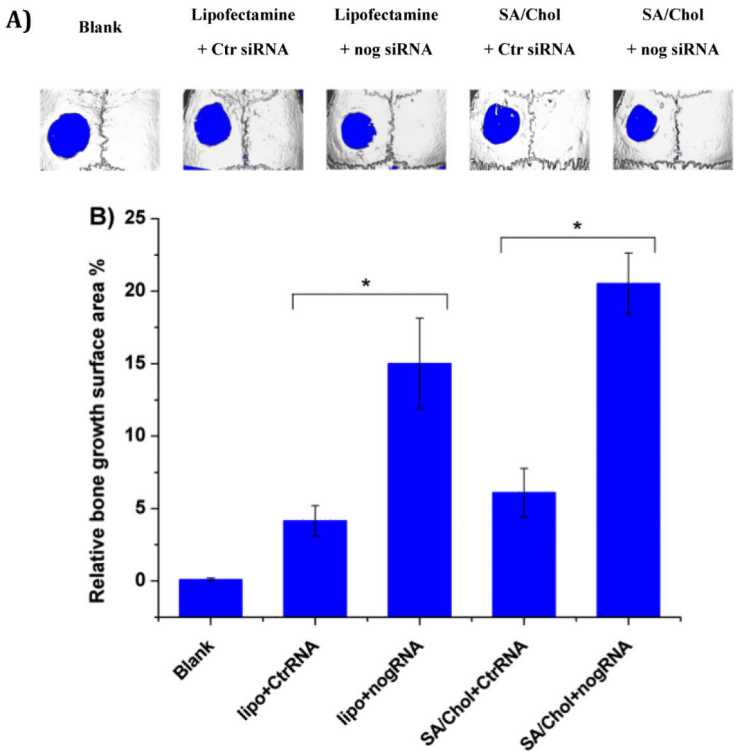

Figure 8.

(A) Micro-computed tomography images of calvarial defects treated with/without MeGC hydrogels encapsulated with ASCs and nanoparticle-siRNA complexes. (B) Quantification of relative bone growth surface area in calvarial defects. Significantly higher bone formation compared with control (*$p < 0.05$).

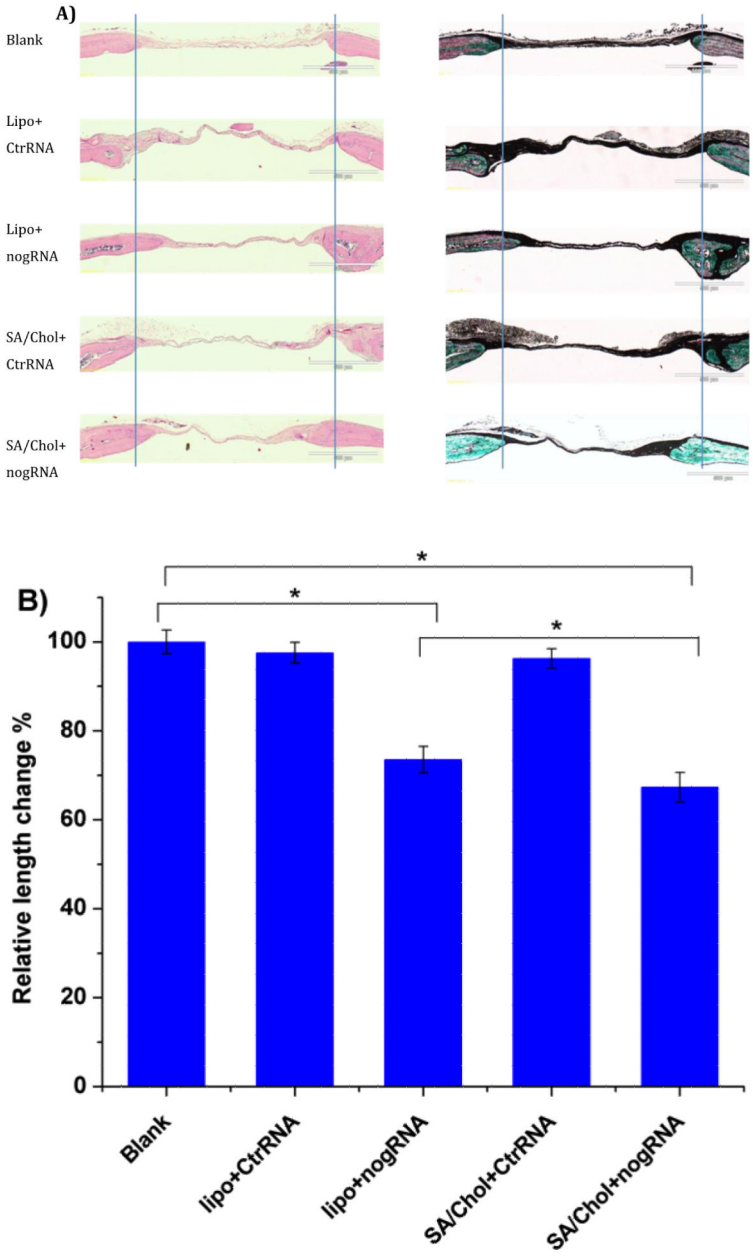

Figure 9.

Histological analysis of bone regeneration in calvarial defects. (A) Hematoxylin-eosin staining (Left), Masson-Goldner trichrome staining (Right), scale bar 500 μm. Two vertical lines were drawn for the ease of observation. (B) The relative length change was measured and normalized to the blank group (n = 4).

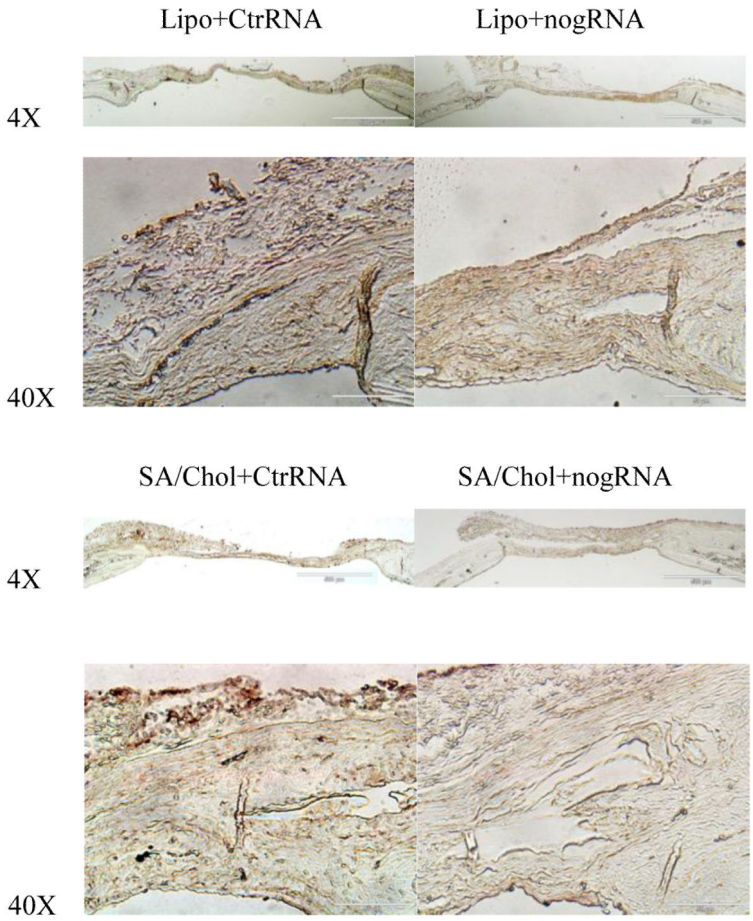

Figure 10.
Immunohistochemical staining of noggin, scale bar 500 μm (4X) and 50 μm (40X).

Table 1

Uptake efficiency of vesicles in various conditions.[a]

Samples	Uptake efficiency
Lipo-siRNA freshly prepared	93.1 ± 1.1%
SA/Chol-siRNA freshly prepared	96.3 ± 1.0%
Lipo-siRNA kept at 37 °C for 14 days	0.2 ± 0.1 %
SA/Chol-siRNA kept at 37 °C for 14 days	62.6 ± 9.4 %

[a] values are mean ± SD.